

# Characterizing semi-interpenetrating polymer networks composed of poly(vinyl chloride) and 5–15% of oligomeric MDI isocyanate cross-linked networks<sup>☆</sup>

C.U. Pittman Jr.<sup>a,\*</sup>, X. Xu<sup>b</sup>, L. Wang<sup>b</sup>, H. Toghiani<sup>b</sup>

<sup>a</sup>Department of Chemistry, Mississippi State University, Box 9573, Mississippi State, MS 39762, USA

<sup>b</sup>Department of Chemical Engineering, Mississippi State University, Box 9573, Mississippi State, MS 39762, USA

Received 19 July 1999; received in revised form 30 September 1999; accepted 4 October 1999

## Abstract

Semi-interpenetrating polymer networks (SIPNs) were prepared from PVC and 5–15 wt.% of di-(4,4-diisocyanatophenyl)methane (MDI) oligomers by directly mixing the liquid MDI with small (150  $\mu\text{m}$  dia.) porous (30% voids) unplasticized PVC particles at low temperatures followed by hot press curing. The tensile, flexural, and impact strengths increased significantly when these small amounts of isocyanate networks were created in PVC. These SIPN blends exhibited  $\tan \delta$  peak temperatures and single distinct loss modulus,  $E''$ , peaks at temperatures lower than those of PVC which had been exposed to the same processing temperatures. These observations rule out the presence of large PVC domains distinct from PVC/isocyanate SIPN domains and pure thermoset domains. A substantial fraction of the isocyanate appears to exist in SIPN type phases in these blends. Considerable amounts of unextracted residue (about 30–36%) remained after 48 h of continuous THF extraction of these SIPN blends. A crude correlation was noticed between the amounts of SIPN residue present and the mechanical strength improvements. Mathematical modeling of DMTA-derived  $T_g$  data by a  $T_g$  third power blend composition equation was employed to understand SIPN structures and the nature of PVC/isocyanate interactions. DMTA measurements of segmental mobility indicated that the isocyanate had a lower cross-link density when diluted in PVC than in the pure cured isocyanate. Fitting experimental  $T_g$  values gave parameters indicating that both the binary hetero-interactions (enthalpic effects) and the conformational redistributions (entropic effects) during the binary hetero-interactions contributed to SIPN formation. © 2000 Elsevier Science Ltd. All rights reserved.

**Keywords:** Poly(vinyl chloride); Oligomeric MDI isocyanate; Semi-interpenetrating polymer networks

## 1. Introduction

Blending high-molecular-weight linear thermoplastics and reactive thermosetting resins is being used increasingly to develop SIPN blends [1–4]. This approach is especially versatile because the degree of blend miscibility is controlled by several factors including the strength of the interaction between components, the mode of reaction between components, the polymers' chemical structures, the stoichiometric composition, and thermoset network cross-linking levels. Recently, we investigated the feasibility of introducing from 5 to 15% by weight of different liquid thermosetting pre-resin compositions into unplasticized,

linear high-molecular-weight PVC at temperatures where PVC is still a solid, followed by curing to cross-link the thermoset resin matrix within the PVC [5]. The objective was to develop a class of semi-interpenetrating polymer networks (SIPNs) by low temperature blending of small PVC porous particles (150  $\mu\text{m}$  dia., 30% void volume as received from the plant) with small weight fractions of liquid thermoset pre-resin components. Upon curing, a cross-linked network diluted in the PVC would form. PVC molecules in such SIPN structures may not be able to disentangle from the cross-linked thermoset network at normal use temperatures. Improvements in the mechanical properties due to the SIPN effects on macromolecular motions occurred. The inclusion of a thermoset network containing functional polar groups within PVC could improve PVC adhesion to fibers or fillers.

Successful SIPN generation via low cost blending of solid, unplasticized PVC at temperatures below pure PVC's glass transition temperature, followed by hot

<sup>☆</sup> A portion of this work was orally presented: X. Xu, L. Wang, H. Toghiani and C.U. Pittman Jr., 54th Southwest Regional ACS Meeting, 1–3 November 1998, Baton Rouge, LA. This work constitutes a portion of the PhD Dissertation of X. Xu, Mississippi State University, 1999.

\* Corresponding author. Tel.: +1-662-325-7616; fax: +1-662-325-7611.

E-mail address: cpittman@ra.msstate.edu (C.U. Pittman Jr.).

molding might seem to be unlikely at first glance. However, several factors combine to give this approach a chance to successfully generate SIPNs. Initial miscibility of isocyanate and PVC arises from the high surface contact area of the small, highly porous PVC particles used as the liquid isocyanate migrates into the pore volume. Interactions between carbonyl or hydroxide groups on the thermosets and the chlorines and  $\alpha$ -hydrogens on the PVC are known to increase miscibility [6]. Thus, liquid MDI oligomers, containing carbonyl oxygens and imino nitrogens, should exhibit favorable enthalpic interactions with PVC to promote miscibility. Next, mixing is promoted by two rolling (dispersive) or high shear mixing. Since the thermoset precursors are small molecules, entropy of mixing provides a driving force for miscibility. However, as these thermoset precursors cure within the PVC, phase separation might be driven by a decrease in the entropy of mixing. PVC chains lose some modes of conformational freedom as the thermoset network forms but gain others, especially if SIPN formation creates more free volume. Thus, the decrease in entropy of mixing occurring during thermoset polymerization might be partially off-set by these factors.

When a small thermoset precursor concentration is dissolved in PVC, the rate of gel formation is decreased by this dilution, becoming slower than in pure thermoset cures. This will have the effect of delaying phase separation while generating a less highly cross-linked thermoset network with longer average segment lengths between cross-links. These more flexible networks should be more compatible with PVC and favor interpenetration. SIPN formation was evident in PVC/thermoset blends based on their mechanical and viscoelastic properties [7] and the thermoset dilution effect played an essential role in SIPN formation.

This paper focuses on further characterizing a PVC/commercial isocyanate blend subset from our earlier work. A PVC/MDI oligomer SIPN blend system was synthesized where the isocyanate content was varied from 3 to 15% by weight. Mechanical testing and dynamic mechanical thermal analysis (DMTA) characterized the structure and viscoelastic properties of these blends. Also, blend extraction analysis provided one measure of SIPN content. A correlation of the amount of SIPN (measured by extraction) to mechanical enhancement revealed that SIPN formation contributed to the mechanical strength enhancements. Furthermore, the SIPN glass transition temperatures were modeled by a third power composition law to help characterize SIPN structural features and the nature of interactions between PVC and isocyanate matrix [8–12].

## 2. Experimental

### 2.1. Materials

Unplasticized PVC (PVC-5225, trade name) was

supplied by Condea Vista Inc. as small, porous particles (150  $\mu\text{m}$  average particle diameter, 30% void volume) direct from the vinyl chloride polymerization. This polymer exhibited  $\eta_{\text{sp}} = 1.56$  (cyclohexanone, 25°C),  $M_n = 53,000$  and  $M_w = 98,000$ . The isocyanate used was PAPI 2027 (trade name), supplied by Dow Chemical Co. PAPI 2027 is an oligomeric MDI isocyanate (isocyanate equiv. wt. 134, functionality 2.7,  $\eta = 0.18$  Pa s at 25°C).

### 2.2. Blend preparation

The low PAPI weight fractions (from 3 to 15% by weight) were used in the PVC/PAPI blends. PAPI 2027 was heated at 65–75°C to reduce its viscosity and permit easy handling. The PVC and the PAPI 2027 were weighed and then premixed in a solid-mixer at a high stirring speed (1000 rpm) at 21–24°C for 1–2 min., followed by continuous blending on a two-roll mill at 50°C until it mixed thoroughly. PAPI 2027 partially fills pores of the PVC particles and some (unquantitated) miscibility occurs which plasticizes PVC. During two-roll milling at 50°C further blending/miscibility occurs but no attempts at quantitating this process was made. Then the blend was pressed into an aluminum mold and cured at 145°C on a hydraulic press under 320–450 atm pressures for 45 min. On heating to 145°C further dissolution of PAPI 2027 into the very soft PVC occurred. However, curing was also taking place.

A pure PVC sample was also hot pressed at 145°C and at about 320 atm for about 45 min in order to compare its properties with those of the SIPNs. A poly(isocyanate) resin sample was made by curing PAPI with water in the air for 3 days at room temperature followed by hot pressing at 145°C and at about 350 atm for 45 min. No additional curing agents were added.

### 2.3. Mechanical property tests

Tensile tests were performed using a Zwick 1435 Universal test machine according to ASTM D638M. Tensile strengths and elongations at break were measured at room temperature. The loadcell was set at 5000 kN, the crosshead speed at 10 mm/min., and the gauge at 25 mm. Three to five separate specimens were measured and the values were averaged. Three-point bending tests were conducted at room temperature on a Zwick 1435 Universal test machine, according to ASTM D790M-I. The loadcell was set at 500 N, the span at 30 mm, and the test speed at 5 mm/min. Flexural properties of each composition were determined from the average value of five to seven test specimens. Izod impact strengths were measured at room temperature on a TMI 45-02 impact tester according to ASTM D256 using a 1 lb. pendulum weight. Five to seven SIPN specimens were tested and the average value was used.

Table 1  
Tensile properties and Izod impact strength of PVC/PAPI SIPNs

PVC/PAPI composition <sup>a</sup> (weight ratio)	Tensile strength <sup>b</sup> (MPa)	Elongation at break (%)	Izod impact strength <sup>c</sup> (J/m)
100/0	15.9 ± 3.7	0.1	21.9 ± 4.4
95/5	25.2 ± 3.3	0.2	32.1 ± 5.4
90/10	28.9 ± 1.9	0.2	39.2 ± 9.1
85/15	22.2 ± 4.8	0.3 ± 0.1	34.7 ± 1.6

<sup>a</sup> Pure PVC samples were molded at 145°C.

<sup>b</sup> Tensile test (ASTM D638M). Loadcell: 5 kN, test speed: 10 mm/min, gauge: 25 mm.

<sup>c</sup> Izod impact test (ASTM D256). Hammer: 1 lb Izod.

#### 2.4. Dynamic mechanical thermal analysis

Storage moduli,  $E'$ , loss moduli,  $E''$ , and loss dissipation factors ( $\tan \delta$ ) were determined in the bending mode using a Polymer Laboratories DMA MK3 instrument. A dual-level bending mode was employed. Small amplitude bending oscillations (both 1 and 10 Hz) were used at a gap setting of 14.00 mm. A heating rate of 2°C/min. was employed over a range from -50 to +170°C. Test specimens were approximately about 1–2 mm thick, 6 mm wide and 45 mm long.

#### 2.5. Blend extraction analysis

A Soxhlet extractor and THF solvent were employed in the extraction experiments at 45°C for 48 h. Three samples of each SIPN blend were extracted and the average undissolved sol–gel content of these samples was obtained. These residues were dried at 60°C and 10 mm Hg for 1 h and the final weight was used to determine the final sol–gel percentage. The pure hot pressed PVC samples were also employed in the extraction experiments under the same conditions in order to compare their extraction behavior with those of SIPN blends.

Table 2  
Flexural properties of PVC/PAPI SIPNs

PVC/PAPI composition <sup>a</sup> (weight ratio)	Flexural strength <sup>b</sup> (MPa)	Flexural modulus (GPa)	Deflection at maximum load <sup>c</sup> (mm)
100/0	26.5 ± 5	1.8 ± 0	0.5 ± 0.1
95/5	50.44 ± 8.5	2.6 ± 0.2	0.9 ± 0.1
90/10	53.2 ± 9.1	2.7 ± 0.2	0.8 ± 0.1
85/15	47.1 ± 6.9	2.7 ± 0.2	0.6 ± 0.1

<sup>a</sup> Pure PVC samples were molded at 145°C.

<sup>b</sup> Three point flexural test (ASTM D790). Loadcell: 500 N, test speed: 5 mm/min, span: 30 mm.

<sup>c</sup> Midspan deflection at maximum loading.

### 3. Results and discussion

#### 3.1. Mechanical properties of PVC/PAPI SIPN blends

The tensile strengths, elongations at break and impact strengths for the PVC/PAPI blends of various compositions are summarized in Table 1. The flexural strengths, flexural moduli, and deflection at maximum loading (3-point bending) for these same blends are summarized in Table 2.

The tensile, flexural and impact strengths and the flexural moduli of the blends were greater than those for PVC in all cases. The elongations at break and the maximum bending deflections also increased. The properties improved most sharply when only 5% PAPI was blended. For example, introducing only 5% PAPI into PVC increased the tensile strength from 15.9 to 25.2 MPa, the impact strength from 21.9 to 32.1 J/m, the flexural strength from 26.5 to 50.4 MPa and flexural modulus from 1.8 to 2.6 GPa. These properties were improved further upon increasing the PAPI content to 10% but the magnitudes of these increases were much less than was obtained upon adding the first 5% PAPI. For example, the tensile strength increased from 25.2 to 28.9 MPa, the impact strength from 32.1 to 39.2 J/m and flexural strength from 50.4 to 53.2 MPa as the PAPI content increased from 5 to 10%. Further increase in PAPI content from 10 to 15% actually lowered the tensile, impact and flexural strengths to 22.2 MPa, 34.7 J/m and 47.1 MPa, respectively.

The mechanical strength improvement, observed when PAPI was added, could result from interpenetration and entanglement of PVC in the PAPI matrices [13,14]. The first 5% thermoset addition gives the largest improvements due to the “dilution effect”. This effect refers to the lower cross-link density (relative to the use of pure isocyanate) which would be generated when small amounts of isocyanate are dissolved within the PVC and then cured. The longer gel time and delay of phase separation may permit more complete SIPN formation per PAPI weight increment within the first 5% PAPI addition than in subsequent additions. Better PVC/PAPI compatibility will exist with the more flexible thermoset segments between cross-links. PAPI’s solubility in PVC is unknown but if a solubility limit exists and is a fairly low value, the fraction of added PAPI which could dissolve would be highest for smaller added weight fractions.

#### 3.2. Dissipation factors ( $\tan \delta$ ) of PVC/PAPI SIPN blends

Plots of the bending dissipation factor ( $\tan \delta$ ) versus temperature at 10 Hz for these PVC/PAPI SIPN blends are shown in Fig. 1, along with that of the PVC which had been hot press molded at 145°C.  $\tan \delta$  peak temperatures at both 1 and 10 Hz are listed in Table 3. PVC exhibits low  $\tan \delta$  values in the glass region (-50 to ~70°C). Then a sharp rise in  $\tan \delta$  occurs as major segmental motions occur between 70 and 95°C. At 10 Hz the  $\tan \delta$  peak occurred at 93°C. At

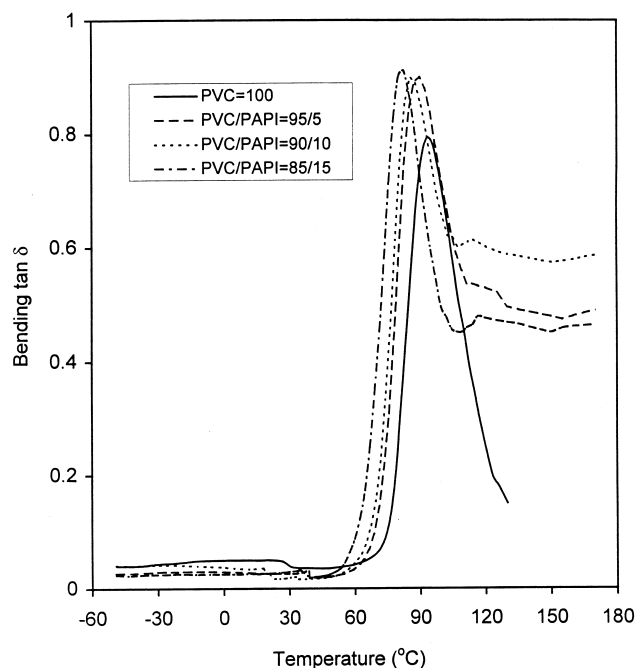


Fig. 1. Dissipation factor ( $\tan \delta$ ) versus temperature of PVC/PAPI SIPN blends at 10 Hz at a heating rate of 2°C/min.

higher temperatures,  $\tan \delta$  values drop with increasing molecular motion.

The  $\tan \delta$  curves of all the PVC/PAPI SIPN blends exhibited maxima at temperatures lower than that for PVC (e.g. <93°C) at all of the PVC/PAPI ratios studied, suggesting that PVC in these regions is plasticized by the PAPI. Lower damping peak temperatures and increased damping peak heights are indications of molecular mixing in blends [15,16]. Perhaps PVC interpenetration of the isocyanate matrix creates greater disorder or induces more free volume in these blends, lowering the  $T_g$ . In addition, each blend exhibited a plateau region above  $T_g$  with the  $\tan \delta$  value lower than the peak temperature but still high. These plateaus can be due to PVC/PAPI regions bound tightly enough within a network so viscous flow/flow energy dissipation cannot operate to lower the value of  $\tan \delta$ . Thus, a preliminary picture emerges that the PVC/PAPI blends have SIPN structures. To various degrees PVC segments are both

plasticized (lower temperature  $\tan \delta$  maxima) and entangled (partially locked) in place (higher temperature  $\tan \delta$  plateau curves).

When the isocyanate segments between cross-links are fairly long, these segments can generate more free volume when in contact with PVC segments. However, the cured isocyanate matrix can still lock PVC chains within by making disentanglement very difficult. The “dilution effect” works to lower the isocyanate network’s cross-link density. Large scale phase separation into PVC and predominantly cross-linked PAPI regions in these blends does not explain the  $\tan \delta$  curves or many of the mechanical property observations. Thus, substantial SIPN type phases seem to be present in these blends. However, very small scale phase-separated domains are still possible. If PVC-rich domains coexisted with more thermoset-rich regions on a domain-size scale of 10–20 nm, a similar  $\tan \delta$  curve could result [17].

### 3.3. Storage moduli, $E'$ , and loss moduli, $E''$ , of PVC/PAPI SIPN blends

Plots of the bending storage moduli ( $E'$ ) and bending loss moduli ( $E''$ ) versus temperature at 10 Hz are shown in Fig. 2, together with those of pure PVC. The temperatures at which the onset of the maximum slope of each plot occurs (one measure of  $T_g$ ) are given in Table 4, along with the  $E''$  peak temperatures for all PVC/PAPI blends.

PVC which had been hot pressed at 145°C exhibited high storage moduli ( $E'$ ) values (>750 MPa) at low temperatures, followed by a catastrophic decrease in modulus of several decades in the vicinity of 65–85°C. Defining  $T_g$  as the temperature of the onset of the maximum slope on the  $E'$  versus temperature curves leads to a  $T_g$  of 81.2°C at 10 Hz for PVC. Defining  $T_g$  as the peak temperature in the loss modulus ( $E''$ ) versus temperature curve gives a  $T_g$  value of 82.5°C at 10 Hz. Above 100°C, both moduli are low and PVC became viscous. PVC also showed a sub- $T_g$  relaxation as shown by both the storage and loss moduli values between ~20 and 45°C well before the  $T_g$  region. This behavior is also exhibited by the blends.

All of the PVC/PAPI blends exhibited the onset of the

Table 3  
Tan  $\delta$  peak temperatures of PVC/PAPI SIPNs at 1 and 10 Hz

PVC/PAPI composition (weight ratio)	$\tan \delta$ peak temperature at 1 Hz (°C)	$\Delta T_{\tan \delta \text{ peak}}$ at 1 Hz (°C) <sup>a</sup>	$\tan \delta$ peak temperature at 10 Hz (°C)	$\Delta T_{\tan \delta \text{ peak}}$ at 10 Hz (°C) <sup>a</sup>
100/0	87.4	0	93.4	0
95/5	81.4	-6	84.9	-8.5
90/10	76.9	-10.5	82.6	-10.8
85/15	82.1	-5.3	85.7	-7.7

<sup>a</sup>  $\Delta T_{\tan \delta \text{ peak}}$  is the difference in temperature between the  $\tan \delta$  peak temperature of pure PVC and that of the SIPN blend at the frequency given. The  $T_g$  value of the thermoset resin, cured PAPI 2027, was 69.8°C ( $\tan \delta$  peak temperature). Pure PAPI was cured to the same 145°C in a hot press at 250 atm (after an initial 3 day room temperature cure to keep out-gassing from disrupting the sample).

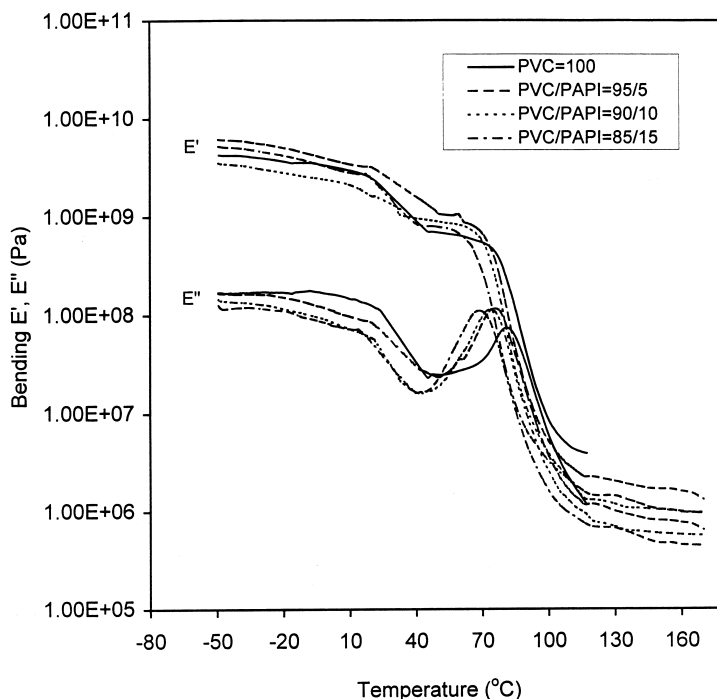


Fig. 2. Temperature dependence of the dynamic storage moduli,  $E'$ , and the dynamic loss moduli,  $E''$ , of PVC/PAPA SIPN blends at 10.0 Hz at a heating rate of 2°C/min.

maximum slope in their storage modulus,  $E'$ , curves at a temperature below the 80°C value for PVC (Fig. 2 and Table 4). These results are in accord with the measured  $\tan \delta$  peak temperatures (at either 1 or 10 Hz) which were also lower for the blends than for PVC. This is evidence that PAPI permeation into the PVC introduces free volume. A similar conclusion is reached by examining the loss moduli,  $E''$ , curves. Every PVC/PAPI blend exhibited a single distinct peak in the  $E''$  versus temperature curves (Fig. 2 and Table 4). Furthermore, each  $E''$  peak temperature was lower than that of the hot press molded PVC. Using the  $E''$  peak temperatures (at 10 Hz) to define the  $T_g$  for the blends, it is clear that PAPI–PVC interactions have lowered the  $T_g$  of each of the blends. Thus, both the  $E'$  and  $E''$  plots, like those of  $\tan \delta$ , are consistent with either a homogeneous SIPN or

SIPNs with some heterogeneity (phase separation) at very tiny domain sizes.

#### 3.4. Correlation of mechanical strength enhancement to unextracted gel fraction

Solvent extraction experiments with THF were conducted to determine if any PVC would remain entangled or tightly bound within the matrices formed upon curing the PVC/PAPI blends. The existence of an SIPN fraction would be proved by such an unextracted residue. First, the pure PVC samples which had been hot pressed at 145°C and 320 atm for 1 h were extracted to establish the behavior of PVC in order to compare it with the blends. Continuous THF extraction at 45°C dissolved almost all of the pure PVC samples. A

Table 4

The temperatures at the onset of the maximum slope of the storage moduli,  $E'$ , versus temperature plots and the peak temperatures of the loss moduli,  $E''$ , versus temperature plots

PVC/PAPI composition (weight ratio)	$T_{\text{at } E' \text{ max.slope at 10 Hz (}^\circ\text{C)}^a}$	$\Delta T_{\text{at } E' \text{ max.slope at 10 Hz (}^\circ\text{C)}^b}$	$T_{E'' \text{ peak at 10 Hz (}^\circ\text{C)}^c}$	$\Delta T_{E'' \text{ peak at 10 Hz (}^\circ\text{C)}^d}$
100/0	81.2	0	82.5	0
95/5	76.3	−4.9	78.5	−4
90/10	72.8	−8.4	77.1	−5.4
85/15	69.7	−11.5	68.5	−14

<sup>a</sup>  $T_{\text{at } E' \text{ max.slope}}$  is the temperature at the onset of the maximum slope in the  $E'$  versus temperature plots of the samples.

<sup>b</sup>  $\Delta T_{\text{at } E' \text{ max.slope}}$  is the difference in this onset of maximum slope temperature between the SIPN blend and PVC.

<sup>c</sup>  $T_{E'' \text{ peak}}$  is the peak temperature of the  $E''$  versus temperature plots.

<sup>d</sup>  $\Delta T_{E'' \text{ peak}}$  is the difference between the  $E''$  peak temperatures of the SIPN blend and PVC.

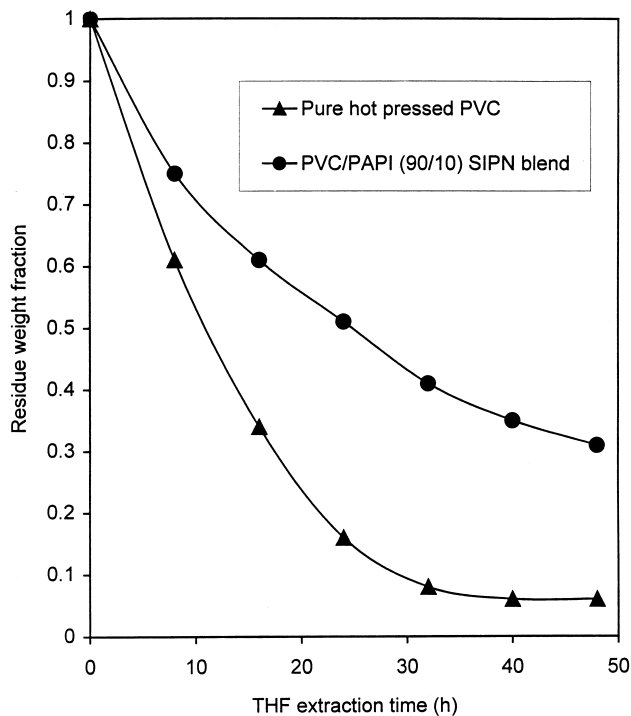


Fig. 3. Extraction of PVC from a PVC/PAPI (90/10) SIPN as a function of extraction time.

small amount of residue remained. This resulted from some HCl elimination and subsequent cross-linking of a very small amount of the PVC during hot pressing. Thus, a small (1–5%) PVC residue would also be expected after THF extraction of the blends. Beyond this small PVC residue, only thoroughly entangled and tightly held PVC molecules could remain within the SIPN blend after 48 h of continuous THF extraction. However, each of the PVC/PAPI SIPN blends exhibited a large amount of residue. The residual sol–gel contents after these 48 h extractions were 36.1% for PVC/PAPI (95/5), 31.9% for PVC/PAPI (90/10), and 31.4% for PVC/PAPI (85/15), respectively. These exhaustive THF extractions demonstrated that substantial amounts of PVC remained entangled or immobilized within PVC/PAPI SIPN phase. These residues confirmed that an SIPN phase had formed which could retain PVC under conditions which strongly favored its removal.

The 48 h extraction experiments do not permit one to know if a single continuous SIPN phase was formed or if very small microphase-separated PVC-rich and PAPI resin-rich domains existed. PVC from PVC-rich domains might extract rapidly into THF leaving behind PVC which was tightly bound/entangled in PAPI resin-rich domains. Alternatively, a continuous single SIPN phase would continually lose PVC during extraction experiments. Therefore, extraction residues were briefly examined as a function of extraction time. Fig. 3 compares the decrease in the

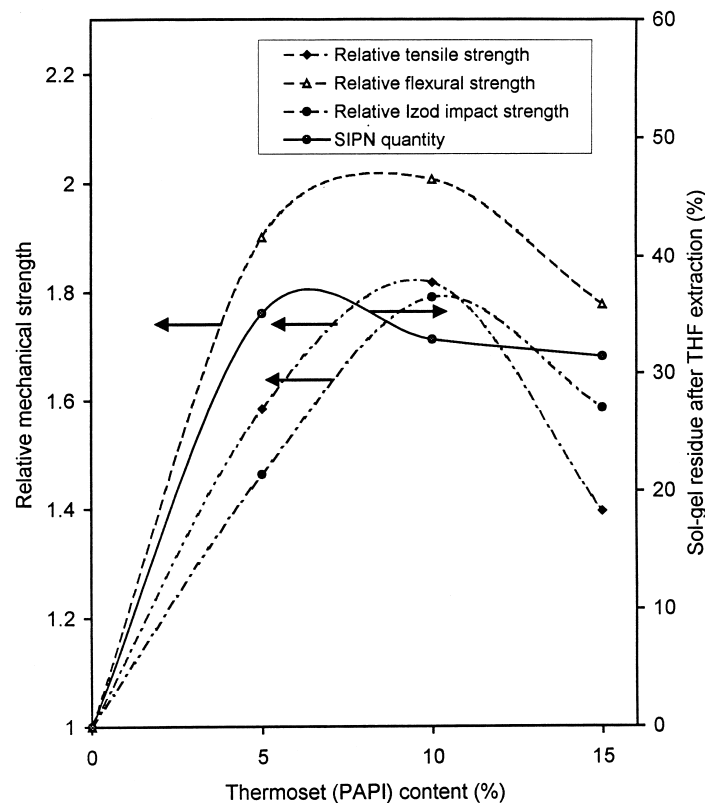


Fig. 4. Correlation between the mechanical strength enhancements and the quantities of sol–gel present after 48 h THF extractions of the PVC/PAPI SIPN blends.

Table 5

Estimation of the segmental mobility ratios for interpenetrated and non-interpenetrating separated network using the Frisch  $T_g$  equation

Weight ratio (PVC/PAPI)	Measured $T_g^a$ (°C)	$T_{g(av.)}^b$ (°C)	$\theta^c$
100/0	87.5	87.5	0
100/3	83.1	86.9	0.05
100/5	81.4	86.6	0.06
100/7	80.1	86.2	0.08
100/9	78.3	85.9	0.1
100/10	76.9	85.7	0.11
100/12	74.1	85.3	0.15
100/14	80.4	84.9	0.06
100/15	82.1	84.8	0.03

<sup>a</sup>  $T_g$  data were taken as the peak temperature in  $\tan \delta$  curves of the samples at 1 Hz from DMTA measurements. The measured  $T_g$  value of pure cured PAPI was about 69.8°C. Pure PAPI was cured to the same 145°C in a hot press at 250 atm (after an initial 3 day room temperature cure to keep out-gassing from disrupting the sample).

<sup>b</sup> Data were obtained using the average  $T_g$  Eq. (1).

<sup>c</sup> Data were obtained using the Frisch  $T_g$  Eq. (2).

weight fraction of the residue versus time for hot pressed pure PVC with that of the PVC/PAPI (90/10) blend. The slower, linear, drop in weight loss is consistent with the presence of a large amount of a continuous SIPN phase. This agrees with a model where most of the PVC was bound/entangled in a diluted PAPI cross-linked resin. The PVC in the PVC/PAPI blend would dissolve more slowly from a SIPN. A faster initial drop due to dissolution from pure PVC domains is not evident in these results but cannot be completely ruled out.

The mechanical strength enhancements were compared to the amount of sol–gel residue obtained after 48 h THF extractions. The relative tensile, impact, and flexural strengths were obtained for each blend by dividing the experimental values by the value of that same quantity obtained from the hot pressed PVC sample. Plots of the relative tensile, impact and flexural strengths versus the percent of sol–gel residue are shown in Fig. 4. A correlation between the amount of sol–gel residue and the three strength improvements is clearly evident. It seems clear that an SIPN effect must be contributing to the mechanical strength enhancements. Thus, semi-interpenetration contributes to the extent of the mechanical strength enhancement.

### 3.5. Evaluation of segmental mobility in PVC/PAPI SIPNs

For those compatible PVC/PAPI blends, the well-known Fox  $T_g$  equation, Eq. (1), was employed to calculate the  $T_g$  values of the PVC/PAPI blends:

$$T_{g(av.)} = W_1 T_{g1} + W_2 T_{g2} \quad (1)$$

$T_{g1}$  and  $T_{g2}$  represent the  $T_g$  values of PVC and cured PAPI, respectively.  $W_1$  and  $W_2$  are the weight fractions of PVC and cured PAPI, respectively.  $T_{g(av.)}$  is the predicted value of  $T_g$  for a blend. The predicted values of  $T_{g(av.)}$  and the measured

values of  $T_g$  (from DMTA) for both the blends and the pure components are listed in Table 5. Clearly, the experimental  $T_g$  values are lower than those of  $T_{g(av.)}$ . The  $T_{g(av.)}$  values from Eq. (1) are based only on the proportions of the two components without any consideration of the interaction between the two components. The calculated value of  $T_{g(av.)}$  can be regarded as the  $T_g$  value for a PVC/PAPI blend where an SIPN has not formed (e.g. a hypothetical non-SIPN blend where PVC does not entangle or interpenetrate with the PAPI network). Thus, the difference between  $T_{g(av.)}$  and the measured  $T_g$  (e.g.  $T_g - T_{g(av.)}$ ) can be attributed to the enhancement of segmental mobility due to SIPN formation.

The Frisch equation [14] can be used to estimate the segmental mobility in the SIPN blends. This equation (see Eqs. (2) and (3)) relates ( $T_g - T_{g(av.)}$ ) to the parameter  $\theta$ .

$$\frac{T_g - T_{g(av.)}}{T_{g(av.)}} = -\frac{\theta}{\theta + 1} \quad (2)$$

$$\theta = \left( \frac{F_x}{F_m} - 1 \right) X'_c \quad (3)$$

$X'_c$  ( $1 > X'_c > 0$ ) represents an increase in physical cross-link density caused by interpenetration within an SIPN.  $F_x$  represents the segmental mobility of the PVC/PAPI SIPN blend while  $F_m$  represents the segmental mobility of a PVC/PAPI blend which is not entangled like an SIPN. The ratio of  $F_x/F_m$  was calculated from Eq. (3).  $F_x/F_m$  represents the ratio of segmental mobilities for the PVC/PAPI SIPN blend versus the non-SIPN blend of PVC/PAPI. Values of  $\theta$  were calculated from the experimental  $T_g$  and calculated  $T_{g(av.)}$  values according to Eq. (2), and they are listed in Table 5. All the  $\theta$  values are shown to be more than zero. Since  $\theta > 0$  and  $X'_c$  has a value between 0 and 1, Eq. (3) requires that  $(F_x/F_m) > 1$ . A positive value of  $\theta$  means that the segmental mobility in the PVC/PAPI SIPNs is larger than in a non-interpenetrating (non-SIPN) of PVC/PAPI. The modeling indicated that PAPI dilution in PVC leads to a lightly cross-linked network with much longer molecular chain segments between cross-links than is present in PAPI cured by itself (absence of PVC). The isocyanate chains between cross-links have much more conformational freedom available than they would if pure PAPI had been cured.

### 3.6. Characterizing the interactions between PVC and PAPI

The  $T_g$  third power concentration equation (Eq. (4)) developed by Brekner et al. [18,19] was used to correlate the experimental  $T_g$  data obtained from PVC–PAPI blends.

$$(T_g - T_{g1})/(T_{g2} - T_{g1}) = (1 + K_1)w_{2c} - (K_1 + K_2)w_{2c}^2 + K_2w_{2c}^3 \quad (4)$$

In Eq. (4),  $T_g$  represents the glass transition temperature of the blend,  $T_{g1}$  and  $T_{g2}$  are the glass transition temperatures of

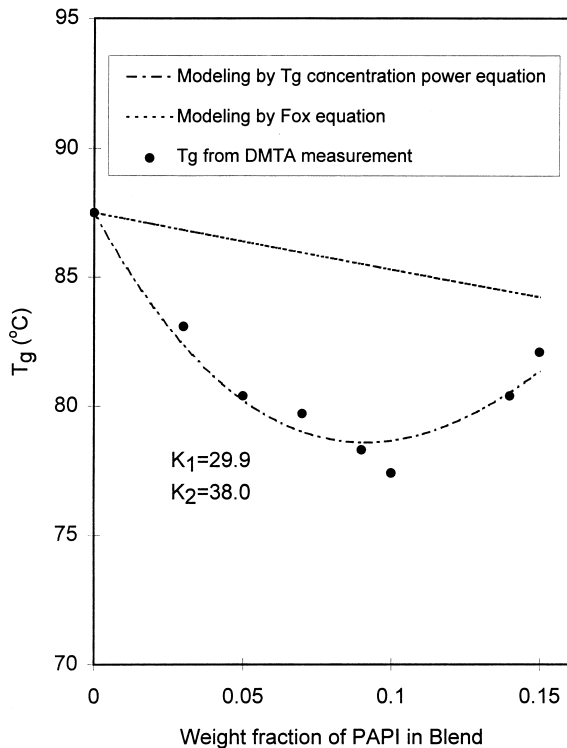


Fig. 5. Modeling the glass transition temperatures of PVC/PAPI SIPN blends.

the two blend components (when pure), respectively.  $K_1$  and  $K_2$  are characteristic parameters of the concentration power equation. The term  $w_{2c}$  is the weight fraction of the component with the higher  $T_{g2}$ , corrected for the different volume expansivities of the blend components. This correction can be expressed as shown in Eqs. (5) and (6).

$$w_{2c} = K_{GT}w_2/(w_1 + K_{GT}w_2) \quad (5)$$

Here,  $K_{GT}$  is the Gordon–Taylor parameter [19], defined as:

$$K_{GT} = (\rho_1/\rho_2)(\Delta\alpha_2/\Delta\alpha_1) \quad (6)$$

where the  $\rho_i$  terms are the densities of the components and the  $\Delta\alpha$  terms are the expansion coefficients at the  $T_g$  values of the components. The weight fraction of the thermoset is  $w_1$ .

Assuming the validity of the Simha–Boyer rule [20] (e.g. that  $\Delta\alpha T_g$  is a constant), the Gordon–Taylor parameter [21] can be expressed as:

$$K_{GT} = (\rho_1/\rho_2)(T_{g1}/T_{g2}) \quad (7)$$

The  $T_g$  concentration power equation was derived [18,19] by assuming that: (1) the binary hetero-contact formation (e.g. molecular contacts between the different polymers of the blend) was driven by enthalpic effects; and (2) the entropy contributions were due to the simultaneously induced conformational redistributions in the neighborhood of the contacts between the two components. To characterize the interactions between the two components, the two characteristic parameters,  $K_1$  and  $K_2$  were introduced into

the  $T_g$  concentration power equation.  $K_1$  and  $K_2$  are defined as shown in Eq. (8) and (9), respectively.

$$K_1 = \{[E_{12-1} + E_{12-2}) - (E_{11-1} + E_{22-2})] - [(e_{12-2} - e_{12-1}) + (e_{11-1} - e_{11-2})]\}/(T_{g2} - T_{g1}) \quad (8)$$

and

$$K_2 = [2e_{12-1} - e_{11-1} - e_{22-1}) - (2e_{12-2} - e_{11-1} - e_{22-2})]/(T_{g2} - T_{g1}) \quad (9)$$

The  $E_{ij-k}$  terms in Eq. (8) represent the interaction energies (enthalpic) stored in a  $ij$  binary contact which must be overcome at the blends'  $T_g$ . This interaction energy (attractive or repulsive) is different than if these interacting lattice sites (in Flory–Huggins terminology) contain the same component. The  $e_{ij-k}$  terms in Eqs. (8) and (9) are the energetic (entropic) contributions to the contact energies, specifically due to the conformational redistributions induced by binary hetero-contact formation (e.g. contact of lattice sites occupied by components 1 and 2, respectively). Therefore,  $K_1$  depends, mainly, on the difference between the interaction energies of the binary hetero-contacts and the homo-contacts (e.g. difference in the lattice interface interaction energies between PVC and PAPI versus PVC/PVC and PAPI/PAPI). If  $K_1 > 0$ , the interactions between the two components of the blend are thermodynamically favorable.  $K_2$  accounts for the additional energetic contribution due to conformational entropy changes during binary hetero-contact formation.

A polynomial regression using the experimental  $T_g$  data for the PVC/PAPI blends was employed in Eq. (4) to estimate  $K_1$  and  $K_2$ . The estimated values of these  $K_1$  and  $K_2$  parameters can help in understanding the nature of PVC–PAPI interactions. The Fox  $T_g$  equation, which was only based on two-composition-additivity, was also employed to model the  $T_g$  versus PAPI composition for the PVC/PAPI system. These modeling results are shown in Fig. 5, which also gives the estimated  $K_1$  and  $K_2$  parameters of Eq. (4).

The predicted  $T_g$  values obtained by fitting the  $T_g$  third power concentration equation matched the experimental data well when  $K_1 = 29.9$  and  $K_2 = 38.0$ . However, the Fox equation did not predict the experimental  $T_g$  data. Comparing the  $T_g$  predictions from the  $T_g$  third power concentration equation with those of the Fox  $T_g$  equation highlights the importance which PVC–PAPI interactions have on glass transition behavior of the SIPN blends.

Both the estimated  $K_1$  and  $K_2$  parameters were positive. As stated in Eq. (9),  $K_1$  mainly depends on the difference between the interaction energies of the binary hetero and homo-contacts. Thus, a positive value of  $K_1$  (i.e.  $[(E_{12-1} + E_{12-2}) - E_{11-1} + E_{22-2})] > 0$ ) indicated that attractive hetero-interaction forces (enthalpic where  $(\Delta H < 0)$ ) between the PVC and PAPI helped to form SIPNs within the blends. During blending, the initial miscibility of the



PAPI precursors and PVC was achieved by the intermolecular Van der Waals, dipole–dipole and hydrogen bonding forces between the PAPI and PVC. In the curing process, the reaction exotherm ( $q < 0$ ) generated during PAPI curing was another thermodynamic driving force promoting miscibility between PVC and PAPI.  $K_2$  reflects contributions due to conformational entropy changes during the formation of binary hetero-contacts between PVC and polyisocyanate segments. The magnitude and sign of the  $K_2$  value for the PVC/PAPI blends illustrates that this entropic contribution is significant and is favorable thermodynamically. Conformational rearrangements between linear PVC and PAPI network segments must occur during SIPN formation. These lead to greater disorder. Thus, one can conclude that the PVC/PAPI SIPN formation was assisted by both the binary hetero-interactions (enthalpic effects) and the conformational redistributions (entropic effects) during these binary hetero-interactions.

#### 4. Conclusions

Semi-interpenetrating polymer networks (SIPNs) composed of PVC and diluted cross-linked PAPI networks were made by introducing small quantities of PAPI (from 5 to 15%) into small-sized, solid, porous PVC particles followed by low temperature roll milling (50°C) and hot press molding at 145°C. The mechanical properties improved for small additions of PAPI into PVC. A substantial amount of an SIPN-like phase must be present in the PVC/PAPI blends according to both DMTA and THF extraction studies. The presence of large PVC-rich domains which are phase separated from thermoset-rich SIPN domains and/or thermoset domains does not fit the data obtained. Tiny microheterogeneous PAPI/PVC regions, which are dispersed in small more PVC-rich regions, cannot be ruled out. The sol–gel residues obtained after THF extractions at 45°C for 48 h confirmed that substantial PVC/PAPI SIPN entanglement remained even after such a vigorous treatment. Mathematical modeling of the glass transition temperatures of PVC/PAPI blends provided an insight into the molecular structural characteristics and nature of interactions between PVC and PAPI components. PAPI, when diluted in PVC, generates a network with a lower cross-link density than the pure cured PAPI would exhibit. Better PVC/PAPI compatibility will exist with more flexible PAPI segments between cross-links. This is

consistent with the enhanced mechanical strengths obtained from the mechanical tests. A  $T_g$  modeling approach to PVC–PAPI interactions, using  $T_g$  a concentration power equation, indicated that the SIPN was formed through both binary hetero-interactions (favorable enthalpic effects) and conformational redistributions (favorable entropic effects) which occur during the binary hetero-interactions.

#### Acknowledgements

This research was supported in part by the National Science Foundation through Grant nos. OSR-9452857 and EPS-9852857. Support from the State of Mississippi and Mississippi State University is gratefully acknowledged. Partial support also was provided by the Air Force Office of Scientific Research, Grant no. F49620-99-1-0191.

#### References

- [1] Su CC, Woo EM. *Polymer* 1995;36:2883.
- [2] Pak SJ, Lyle GD, Mercier R, McGrath JE. *Polymer* 1993;34:885.
- [3] Pearson RA, Yee AF. *Polymer* 1993;34:3658.
- [4] Hsieh HK, Woo EM. *J Polym Sci, Polym Phys Ed* 1996;34:2591.
- [5] Xu X, Wang L, Toghiani H, Pittman CU, Jr. Phase behavior of poly(vinyl chloride)/polyurethane blends. 54th Southwest regional ACS Meeting, 1–3 November 1998, Baton Rouge, LA.
- [6] Kim SJ, Kim BK, Jeong HM. *J Appl Polym Sci* 1994;51:2187.
- [7] Pittman Jr. CU, Xu X, Wang L, Toghiani H. *Polym Eng Sci* 1999 in press.
- [8] Kumar A, Gupta RK, editors. *Fundamentals of polymers* New York: McGraw-Hill, 1998 chap. 8.
- [9] Ramos AR, Cohen RE. *Polym Eng Sci* 1977;17:639.
- [10] Frisch HL, Klempner D, Frisch KC. *J Appl Polym Sci* 1974;18:683.
- [11] Klempner D, Frisch HL, Frisch KC. *J Polym Sci A* 1972;8(2):921.
- [12] Matsuo M, Kwei TK, Klempner D, Frisch KC. *Polym Eng Sci* 1970;10:327.
- [13] Sperling LH, Friedman H. *J Appl Polym Sci A* 1969;7(2):425.
- [14] Frisch HI, Frisch KC, Klempner D. *Polym Eng Sci* 1974;14:648.
- [15] Inoue T. *Prog Polym Sci* 1995;20:119.
- [16] Ramos AR, Cohen RE. *Polym Eng Sci* 1977;17:639.
- [17] Klempner D, Sperling LH, Utracki LA, editors. *Interpenetrating polymer networks* Washington, DC: American Chemical Society, 1994. pp. 12–20.
- [18] Brekner MJ, Schneider HA, Cantow HJ. *Makromol Chem* 1988;189:2085.
- [19] Brekner MJ, Schneider HA, Cantow HJ. *Polymer* 1988;29:2085.
- [20] Simha R, Boyer RF. *J Chem Phys* 1962;37:1003.
- [21] Vilics T, Schneider HA, Manovicu V, Manovicu I. *Polymer* 1997;38(8):1865.